

Author Manuscript

Faculty of Biology and Medicine Publication

This paper has been peer-reviewed but does not include the final publisher proof-corrections or journal pagination.

Published in final edited form as:

Title: 2-Arachidonoylglycerol mobilizes myeloid cells and worsens heart function after acute myocardial infarction.

Authors: Schloss MJ, Horckmans M, Guillamat-Prats R, Hering D, Lauer E, Lenglet S, Weber C, Thomas A, Steffens S

Journal: Cardiovascular research

Year: 2019 Mar 1

Issue: 115

Volume: 3

Pages: 602-613

DOI: 10.1093/cvr/cvy242

In the absence of a copyright statement, users should assume that standard copyright protection applies, unless the article contains an explicit statement to the contrary. In case of doubt, contact the journal publisher to verify the copyright status of an article.

2-arachidonoylglycerol mobilizes myeloid cells and worsens heart function after acute myocardial infarction

Maximilian J. Schloss^{1*}, Michael Horckmans^{1,2*}, Raquel Guillamat-Prats¹, Daniel Hering¹, Estelle Lauer³, Sébastien Lenglet³, Christian Weber^{1,4,6}, Aurelien Thomas^{3,5}, Sabine Steffens^{1,6}

¹Institute for Cardiovascular Prevention (IPEK), Ludwig-Maximilians-University (LMU) Munich, Germany; ²Institut de Recherche Interdisciplinaire en Biologie Humaine et Moléculaire (IRIBHM), Université Libre de Bruxelles (U.L.B.), Brussels, Belgium; ³Unit of Toxicology, CURML, Lausanne University Hospital, Geneva University Hospitals, rue Michel-Servet 1, CH-1211 Geneva, Switzerland; ⁴Dept. of Biochemistry, Cardiovascular Research Institute Maastricht (CARIM), Maastricht University, The Netherlands; ⁵Faculty of Biology and Medicine, University of Lausanne, Vulliette 04, 1000 Lausanne, Switzerland; ⁶German Centre for Cardiovascular Research (DZHK), partner site Munich Heart Alliance, Munich, Germany

*equally contributing first-authors

Short title: endocannabinoids regulate myeloid cell recruitment

Total word count: 8'206

Address correspondence to:

Sabine Steffens, PhD, FESC

Institute for Cardiovascular Prevention, Pettenkoferstr. 9, 80336 Munich, Germany

Phone: +49 (0)89 4400 54674

email: sabine.steffens@med.uni-muenchen.de

Abstract

Aims: Myocardial infarction leads to an enhanced release of endocannabinoids and a massive accumulation of neutrophils and monocytes within the ischemic myocardium. These myeloid cells originate from hematopoietic precursors in the bone marrow and are rapidly mobilized in response to myocardial infarction. We aimed to determine whether endocannabinoid signaling is involved in myeloid cell mobilization and cardiac recruitment after ischemia onset.

Methods and results: Intravenous administration of endocannabinoid 2-arachidonoylglycerol into wildtype C57BL6 mice induced a rapid increase of blood neutrophil and monocyte counts as measured by flow cytometry. This effect was blunted when using cannabinoid receptor 2 knockout mice. In response to myocardial infarction induced in wildtype mice, the lipidomic analysis revealed significantly elevated plasma and cardiac levels of the endocannabinoid 2-arachidonoylglycerol 24 h after infarction, but no changes in anandamide, palmitoylethanolamide and oleoylethanolamide. This was a consequence of an increased expression of 2-arachidonoylglycerol synthesizing enzyme diacylglycerol lipase and a decrease of metabolizing enzyme monoacylglycerol lipase in infarcted hearts, as determined by quantitative RT-PCR analysis. The opposite mRNA expression pattern was observed in bone marrow. Pharmacological blockade of monoacylglycerol lipase with JZL184 and thus increased systemic 2-arachidonoylglycerol levels in wildtype mice subjected to myocardial infarction resulted in elevated cardiac CXCL1, CXCL2 and MMP9 protein levels as well as higher cardiac neutrophil and monocyte counts 24 h after infarction compared to vehicle-treated mice. Increased post-myocardial infarction inflammation in these mice led to an increased infarct size, an impaired ventricular scar formation assessed by histology and a worsened cardiac function in echocardiography evaluations up to 21 days. Likewise, JZL184-administration in a myocardial ischemia-reperfusion model increased cardiac myeloid cell recruitment and resulted in a larger fibrotic scar size.

Conclusions: These findings suggest that changes in endocannabinoid gradients due to altered tissue levels contribute to myeloid cell recruitment from the bone marrow to the infarcted heart, with crucial consequences on cardiac healing and function.

Key words: myocardial infarction, monocytes, neutrophils, monoacylglycerol lipase, CB2 cannabinoid receptor

1. Introduction

The endocannabinoid system is a regulatory lipid signaling system that is involved in the homeostatic control of many physiological processes. These include the regulation of immune cell function, which is mainly attributed to cannabinoid receptor 2 (CB2) signaling.¹ The most abundant endogenous CB2 agonist is 2-arachidonoylglycerol (2-AG), which is produced on demand from membrane phospholipids in many tissues, including bone marrow,² spleen,³ blood and heart.⁴ The major biosynthesizing enzyme for 2-AG is diacylglycerol lipase (DAGL) and its metabolism to arachidonic acid and glycerol occurs through the catalytic activity of monoacylglycerol lipase (MAGL).⁵ CB2 deficiency in mice (CB2^{-/-}) leads to exaggerated myocardial ischemia-reperfusion injury and unfavorable post-myocardial infarction (MI) healing.⁶⁻⁹ The beneficial effects of CB2 signaling in this setting involve cardioprotective mechanisms as well as anti-fibrotic and anti-inflammatory effects.^{6,7,10} CB2 is most abundantly expressed on immune cells, including myeloid cells.¹ Stimulation of CB2 has been reported to regulate leukocyte recruitment, both directly via chemoattraction and indirectly through inhibition of chemokine-induced recruitment.¹¹ Thus, CB2 signaling might play a dual role by either promoting local recruitment to inflammatory sites or by limiting immune cell recruitment and thus dampening an ongoing inflammatory response.

MI leads to necrosis of a large number of cardiomyocytes, which induces a rapid infiltration of immune cells such as neutrophils and monocytes. Substantial progress has been made over the past few years in understanding their role in MI healing. These innate immune cells are instrumental in clearing the infarct area from tissue debris and subsequently promoting angiogenesis and fibrosis. The inflammatory response needs to be well-balanced, as an excessive number or a persistent presence of immune cells may lead to an unresolved resolution of inflammation. Consequently, the process of granulation tissue and collagen formation would be disturbed, which could promote cardiac dysfunction.^{12, 13} Conversely, in the case of insufficient numbers of immune cells, infarct healing is delayed because dead cells are not removed and repair processes not properly induced.¹²⁻¹⁴ Under homeostatic conditions, myeloid cells are produced and stored in the bone marrow and spleen, from where they are rapidly mobilized after an acute MI. In view of a potential role of endocannabinoid signaling in leukocyte retention in the bone marrow niche, 2-AG levels have been reported to be much higher in bone marrow and spleen compared to plasma, suggesting a homeostatic gradient.² On the other hand, tissue injury leads to a significant increase in blood and organ endocannabinoid levels.¹⁵⁻¹⁷

Here, we studied the role of endocannabinoid 2-AG signaling in myeloid cell mobilization and recruitment during homeostasis and in response to cardiac injury in mice. Our data reveal that 2-AG induces myeloid cell mobilization into the blood, which is blunted in absence of CB2. MI increases systemic and cardiac 2-AG levels by shifting the expression profile of 2-AG biosynthesizing and degrading enzymes between bone marrow and infarcted myocardium, thereby promoting a gradient favoring myeloid cell recruitment to the injured heart. Blocking of the MAGL pathway in mice subjected to MI increased cardiac myeloid cell infiltration and inflammation, leading to increased infarct sizes, impaired cardiac wound healing and worsened cardiac function.

2. Methods

2.1 Animal experiments

Female 10- to 12-week-old C57BL/6J (wildtype, WT) and cannabinoid receptor (CB2^{-/-})¹⁸ mice (with constitutive knockout of the gene encoding CB2) were used in this study. Mice were bred and housed under controlled conditions in a 12 h light/12 h dark cycle. For leukocyte mobilization experiments under steady state, mice received intravenous injections of 10 mg/kg 2-arachidonoylglycerol (Tocris).¹⁹ MI was induced by permanent ligation of the left anterior descending coronary artery (LAD). Selective experiments were performed in mice subjected to transient 45 min of myocardial ischemia followed by 24 h or 7 days of reperfusion. Sham-operated animals were submitted to the same surgical protocol as described below but without LAD occlusion. Mice were first randomized and then underwent either sham- or I/R-surgeries on the same day alternating between both surgeries to prevent any procedural or time-of-surgery bias. Sham- and MI-operated mice were harvested together 24h after surgery and all subsequent experiments of both groups were performed together. For the MI surgeries, mice were anesthetized with midazolam (5 mg/kg), medetomidin (0,5 mg/kg) and fentanyl (0,05 mg/kg), intubated and ventilated with a MiniVent mouse ventilator (Harvard Apparatus, Holliston, MA). A left thoracotomy was performed in the 4th left intercostal space, and the pericardium was carefully incised to maintain the integrity of the pericardial adipose tissue. MI was induced by permanent or transient ligation of the LAD distal to its bifurcation from the main stem with monofilament nylon 7-0 sutures (Ethicon, Somerville, USA). The chest wall and skin were closed with 5-0 nylon sutures (Ethicon, Sommerville, NJ). After surgery, naloxone (1,2 mg/kg), flumazenil (0,5 mg/kg) and atipamezol (2,5 mg/kg) were injected to reverse the effect of anesthesia. Post-operative analgesia (buprenorphine; 0,1 mg/kg) was given for the first 12 h

after surgery. In selective experiments, mice received intraperitoneal injections of MAGL inhibitor JZL184 (16mg/kg; CAS 1101854-58-3; Cayman Chemical) or corresponding vehicle (5% DMSO in saline) one day before LAD ligation, followed by injections at day 1, 3, 5, 7, 9, 11, 13, 15, 17, 19 and 21 after LAD occlusion (or until harvest). At the end of the experiment, mice were euthanized by intraperitoneal injection of anesthesia overdose (90 mg/kg ketamine, 6 mg/kg xylazine) and subsequent exsanguination via cardiac puncture followed by perfusion with phosphate buffered saline. All animal experiments were approved by the local ethical committee and are in accordance with the guidelines from Directive 2010/63/EU of the European Parliament on the protection of animals used for scientific purposes.

2.2 Echocardiography

Transthoracic echocardiography was performed before and 3, 7, 14 and 21 days after MI on mildly anesthetized spontaneously breathing mice (sedated by inhalation of 1% isoflurane, 1 L/min oxygen), using a Vevo 3100 High Resolution Imaging system (Visualsonics, Toronto, Canada). The mice were placed on a heated ECG platform and left parasternal long axis view and left mid-papillary short axis views were acquired in B-Mode and M-Mode, respectively. End-diastolic volumes, end-systolic volumes, stroke volumes, ejection fractions and fractional shortening were evaluated on the left parasternal long axis view. The left ventricular anterior wall thickness was measured on the left mid-papillary short axis view in systole and diastole and the average between heart cycles was calculated. Vector displacement and 3-D wall displacement were generated and cardiac output was calculated using the Vevo software.

2.3 Infarct size and mortality

Hearts were perfused and harvested 24 h after LAD ligation and sectioned into 4 equal transverse slices. The slices were incubated in 2% triphenyltetrazolium chloride (TTC) solution (Sigma-Aldrich) at 37°C for 15 min and fixed overnight in 4% formalin at 4°C. Images were taken at 10x magnification, and quantification of viable (red) and infarct areas (white) was performed in a blinded manner with Image J software. Each mouse, which died after surgery prior to organ harvest underwent thoracotomy for post-mortem investigation if a cardiac rupture with intrapericardial hemorrhage had occurred.

2.4 Histology

Four-micrometer paraffin heart sections were stained with Masson's trichrome as follows: sections were rehydrated and incubated in heated Boin's solution before staining in Weigert's

iron hematoxylin and Biebrich scarlet-acid fuchsin solution. After transferring to phosphotungstic/phosphomolybdic acid and subsequent staining with aniline blue, sections were dehydrated and mounted with Entellan® (Sigma-Aldrich). Fibrosis was quantified as the relative area of blue staining (collagen) compared to the left ventricle surface, as an average of 3–4 sections per heart at the level of the papillary muscle, using ImageJ software.²⁰ Remnants of pericardial tissue around the heart were excluded from fibrosis quantification. The anterior wall thickness of the left ventricle was measured on Masson's trichome-stained sections as an average of 3–4 sections per heart. For Sirius Red staining of collagen, 3–4 sections per heart were incubated for 40 min with 0.1% Sirius Red (Sigma-Aldrich). Sections were photographed with identical exposure settings under ordinary polychromatic or polarized light microscopy. Interstitial collagen subtypes were evaluated using polarized light illumination; under this condition, thicker type I collagen fibers appeared orange or red, whereas thinner type III collagen fibers were yellow or green. TUNEL staining was performed with paraffin-embedded heart sections to evaluate apoptosis in the infarcted area according to the manufacturer's instructions (DeadEnd™ Fluorometric TUNEL System, Promega). Sections were counterstained with DAPI (Fluoroshield mounting medium, Abcam) and mounted with cover slip. Images (10x magnification fields within infarct areas, 2-3 fields per section) were taken using a Leica DM6000 microscope and the analysis was performed using the Leica Application Suite LAS V4.3 software unless otherwise indicated.

2.5 Cytokine and chemokine measurements

Plasma chemokines and cytokines were measured with ProcartaPlex™ Multiplex immunoassay (eBioscience). Troponin I levels were measured with a precoated enzyme-linked immunosorbent assay (ELISA kit, CUSABIO). CXCL12 levels in bone marrow lavage of femurs (flushed with 1 ml PBS per femur) were determined with standard ELISA (Duoset, R&D Systems). Approximately 30 mg tissue dissected from infarct areas (apex region) were lysed in protein lysis buffer (50 mM Tris, 150 mM NaCl pH 8.0, 0.1% Triton X 100, 0.5% sodium deoxycholate, supplemented with protease inhibitor cocktail, Roche) using a tissue homogenizer (TissueLyser LT, Qiagen). Finally, cardiac chemokines were measured with standard ELISA kits (Duoset, R&D Systems) and protein concentrations in cardiac lysates were determined by Bradford Coomassie brilliant blue assay (Biorad).

2.6 Blood Counter

Freshly obtained EDTA blood harvested by cardiac puncture was used to analyze leukocyte counts using an animal blood counter (scil Vet ABC Hematology Analyzer).

2.7 Flow cytometry of heart and bone marrow

Hearts were harvested, perfused with saline to remove peripheral cells, minced with fine scissors, and digested with collagenase I (450 U/ml), collagenase XI (125 U/ml), hyaluronidase type I-s (60 U/ml) and DNase (60 U/ml; Sigma-Aldrich and Worthington Biochemical Corporation) at 37°C for 1 h. Bone marrow cells were obtained by flushing femurs with 2 ml of saline and triturated through 70 µm nylon mesh strainer. The resulting single cell suspensions were centrifuged, resuspended in PBS supplemented with 1% BSA and CD16/CD32 Fc-block and incubated with following monoclonal antibodies for 30 min at 4°C at 1/1000 dilution: anti-CD45.2 (clone 104, BD Biosciences), anti-CD11b (clone M1/70, BioLegend), anti-Ly6G (clone 1A8, BioLegend), anti-F4/80 (clone BM8, BioLegend), and isotype controls (BioLegend). Anti-CD115 (clone AFS98, BioLegend) and anti-CD206 (clone C068C2, BioLegend) were used at 1/500 dilution. Neutrophils were identified as CD45+, CD11b+, Ly6G+; blood monocytes as CD45+, CD11b+, Ly6G-, F4/80-, CD115+ and further gated for Ly6C^{high} and Ly6C^{low} expressing subpopulations; cardiac monocytes as CD45+, CD11b+, Ly6G-, F4/80- and further gated for the Ly6C^{high} expressing subpopulation (*Supplemental Figure 1*); cardiac macrophages as CD45+, CD11b+, Ly6G-, F4/80+ and further gated for CD206- for M1 subpopulation and CD206+ for M2 subpopulation. Data were acquired on a FACS Canto II (BD Biosciences), and analysis was performed with FloJo software (Ashland, USA).

2.8 Quantitative real time RT PCR

Whole RNA from lysed hearts (TissueLyser LT, Qiagen) or bone marrow cells was extracted (peqGold Trifast and Total RNA kit, Peqlab) and reverse transcribed (PrimeScript™ RT reagent kit, Clontech). Real-time PCR was performed with the 7900HT Sequence Detection System (Applied Biosystems) using the KAPA PROBE FAST Universal qPCR kit (Peqlab) unless otherwise indicated and predesigned primer and probe mix (DAGL-β, Mm00523381_m1; Vcam1, Mm01320970_m1; TaqMan® Gene Expression Assays, Life Technologies) as well as custom primers and probes (Supplemental Table 1; Eurofins Genomics). Real time PCR analysis of Mmp9 was performed with SYBR Green Master Mix (Applied Biosystems) and custom primers (Supplemental Table 1). Messenger RNA expression

of markers of interest was normalized to hypoxanthine-guanine phosphoribosyltransferase (HPRT), and the fold induction was calculated by the comparative C_t method.

2.9 Western Blotting

The cardiac infarct area was excised and lysed in RIPA buffer (50 mM Tris, 150 mM NaCl, 1% Triton X-100, 0.5% sodium deoxycholate, 0.1% SDS, pH 8.0) supplemented with a protease inhibitor cocktail (Complete Mini, Roche) using a tissue homogenizer (TissueLyser LT, Qiagen). Aliquots (30 µg) of total protein were separated by SDS-polyacrylamide gel electrophoresis and transferred to nitrocellulose membranes. After blocking for 1 h in Tris-buffered saline containing 0.1% Tween 20 and 5% skim milk (Carl Roth), membranes were probed overnight at 4°C with primary antibody against MMP-9 (R&D, MAB911; 1/2000 dilution) or 60 min for GAPDH (Sigma-Aldrich, G954; 1/10000). Densitometric quantification of protein bands was performed using ImageJ software (NIH, Bethesda, MD, USA) and MMP9 expression was normalized to GAPDH.

2.10 Endocannabinoid tissue measurements

Endocannabinoids were extracted from 100 µl of plasma or 10 mg cardiac tissue by liquid-liquid extraction, and then separated by liquid chromatography (Ultimate 3000RS, Dionex, CA, USA). Analyses were performed on a 5500 QTrap® triple quadrupole/linear ion trap (QqQLIT) mass spectrometer equipped with a TurboIon-SprayTM interface (AB Sciex, Concord, ON, Canada).^{21, 22}

2.11 Statistical analysis

Comparisons between two groups of normally distributed and not connected data were performed using the unpaired Student's t-test. Comparisons between two groups of normally distributed and connected data were performed using the paired Student's t-test. Comparisons between multiple group comparisons were performed by two-way ANOVA followed by Bonferroni post-hoc test. Mortality was analyzed by log-rank test. All data are expressed as mean ± SEM, and statistical analysis was performed with Prism Software (version 7; GraphPad, CA). P<0.05 was considered significant.

3. Results

3.1 Endocannabinoid 2-AG induces myeloid cell mobilization into the circulation

In order to test whether an increase in circulating endocannabinoid 2-AG levels might induce myeloid cell mobilization from hematopoietic reservoirs into the circulation, we injected a bolus of 2-AG (10 mg/kg) intravenously into WT mice. The comparison of blood counts before and 2 h after 2-AG administration in same animals revealed at least 2-fold higher circulating numbers of neutrophils and monocytes (both Ly6C^{high} and Ly6C^{low} populations) after 2-AG injection (*Figure 1*). To clarify whether the release into the blood was mediated via CB2 receptors, we repeated the same experiment in CB2^{-/-} mice. In support of a crucial role for CB2 signaling in myeloid cell mobilization, systemic 2-AG administration failed to increase monocyte counts and raised only 1.3-fold neutrophil counts in these mice (*Figure 1*). However, we noticed that circulating blood neutrophil counts per se were higher in CB2^{-/-} compared to WT mice (WT $0,78 \times 10^6/\text{ml} \pm 0,08$; CB2^{-/-} $1,21 \times 10^6/\text{ml} \pm 0,11$ at baseline; $P < 0.05$). We hypothesized that elevated blood neutrophil counts in CB2^{-/-} mice at baseline might be a consequence of alterations in factors regulating homeostatic granulocyte retention in the bone marrow. Indeed, we found slightly lower neutrophil counts in the bone marrow of CB2^{-/-} mice (*Supplemental Figure IIA*). This phenotype was accompanied by reduced bone marrow levels of CXCL12 (*Supplemental Figure IIB*), a chemokine released by stromal cells to retain neutrophil progenitors and mature neutrophils at their site of production. Moreover, we detected a 50% lower VCAM-1 mRNA expression in lysates of hematopoietic bone marrow cells obtained from CB2^{-/-} compared to WT mice (*Supplemental Figure IIC*). Thus, reduced expression of VCAM-1, which binds to integrins expressed by neutrophils, might contribute to enhanced neutrophil egress from the bone marrow.

3.2 MI induces an inverted expression profile of endocannabinoid synthesizing and metabolizing enzymes between bone marrow and heart

To clarify whether endocannabinoid levels might be systemically induced after MI in our mouse model, we quantified various endocannabinoids and related lipid mediators in the plasma and myocardium of non-infarcted versus infarcted WT mice. We found that only 2-AG was upregulated in hearts and plasma 24 h after MI, while anandamide, palmitoylethanolamide and oleoylethanolamide were not changed (*Figure 2A-B*). We further compared tissue mRNA levels of enzymes involved in 2-AG biosynthesis and metabolism between steady state and 24 h after MI. Cardiac levels of endocannabinoid 2-AG producing enzyme DAGL-β were 2-fold higher 24 h after MI compared to baseline (*Figure 2C*), whereas its bone marrow expression levels decreased (*Figure 2D*). Conversely, mRNA levels of the enzyme MAGL which metabolizes 2-AG were significantly downregulated in ischemic myocardium (*Figure 2C*), but massively

upregulated in the bone marrow (*Figure 2D*). Similar expression patterns were observed in CB2^{-/-} mice (*Supplemental Figure III*). Thus, our data indicate that MI leads to an altered 2-AG gradient between bone marrow, plasma and heart due to a modulation of tissue and plasma levels, which may promote leukocyte mobilization.

3.3 Pharmacological blockade of 2-AG metabolism enhances cardiac neutrophil and monocyte recruitment and inflammation

To further clarify the causal implication of 2-AG in post-MI myeloid cell recruitment, we treated mice with a pharmacological inhibitor of the 2-AG degrading enzyme MAGL (JZL184) or with the corresponding vehicle (DMSO) (*Figure 3A*). Blood counter analysis 24 h after MI revealed significantly higher circulating granulocyte and monocyte counts in mice receiving MAGL inhibitor compared to vehicle-treated mice (*Figure 3B*). The effect on cardiac myeloid cell infiltrates was even more impressive, revealing at least 2-fold higher cardiac neutrophil and inflammatory Ly6C^{high} monocyte counts in JZL184- compared to vehicle-treated mice (*Figure 3C*). Concomitantly, protein levels of neutrophil recruiting chemokines CXCL1 and CXCL2 within the infarcted myocardium were significantly elevated in JZL184-treated mice 24 h after MI, while levels of monocyte recruiting chemokine CCL2 were not significantly different compared to the vehicle-treated mice (*Figure 3D*). Infiltrated neutrophils release their granule proteins such as MMP9, which may further contribute to cardiac tissue damage in addition to the primary ischemic event. In line with increased neutrophil counts in hearts of JZL184-treated mice, Western blot analysis confirmed significantly higher cardiac MMP9 protein levels at the same time point (*Figure 3E-F*).

The increase in cardiac cytokine levels was accompanied by increased plasma levels of the inflammatory cytokine TNF α in JZL184-treated mice 24 h after MI (*Figure 3G*), whereas CXCL1, CXCL2 and CCL2 plasma levels were not significantly higher (*Figure 3H*).

3.4 Pharmacological MAGL-inhibition increases infarct size and mortality

In agreement with enhanced inflammatory cell recruitment, mice receiving MAGL inhibitor had significantly larger infarct sizes quantified by TTC staining 24 h after permanent LAD occlusion (*Figure 4A-B*). Troponin I plasma levels 24 h after MI were not significantly different between both groups, possibly because this time point of analysis was beyond the plasma peak of this clinical marker (*Figure 4C*). Survival analysis after MI revealed a slightly higher mortality with increased incidences of ventricular ruptures in JZL184-treated mice compared with the vehicle group (*Figure 4D-E*).

3.5 Pharmacological MAGL-inhibition impairs ventricular remodeling 7d after MI

To investigate the consequences of 2-AG driven inflammation on post-MI wound healing and remodeling, we subjected mice treated with either vehicle or MAGL inhibitor to permanent LAD ligation and performed analysis of hearts after 7 days. Immunhistological TUNEL staining and subsequent analysis of apoptotic cells within the infarct area showed no differences between vehicle- and JZL184-treated mice (*Figure 5 A-B*). To study the effect of JZL184 treatment on cardiac fibrosis we performed Masson's trichrome staining of infarcted hearts. JZL184-treated mice had larger ventricular scars with a significantly thinner left ventricular anterior wall thickness than vehicle-treated mice (*Figure 5 C-D*). Sirius red staining and subsequent analysis of the collagen composition within the infarcted myocardium revealed a significantly lower density of thick collagen type I fibers in JZL184-treated mice compared to the vehicle group (*Figure 5 E-F*). Larger fibrotic scars and less collagen type 1 fibers might be contributing factors for the higher incidence of ventricular ruptures in the JZL184-treated mice.

3.6 Pharmacological MAGL-inhibition worsens cardiac function after MI

Since enhanced inflammation and impaired wound healing may have detrimental effects on post-MI outcome, we performed additional experiments to study prolonged effects of MAGL inhibition on cardiac function parameters. Echocardiographic analysis of vector displacement of ventricular walls, which indicates ventricular wall movement, appeared more reduced in JZL184-treated mice 14 days after MI (*Figure 6A*). The quantification of echocardiographic measurements revealed massively reduced ejection fractions 3 to 21 days post-MI in both experimental groups, with a significantly more pronounced decline in JZL184-treated mice (*Figure 6B*). In parallel, there was a continuous increase of the end-systolic and end-diastolic volumes, which was significantly more pronounced in JZL184-treated mice 14 and 21 days after MI compared to the vehicle group (*Figure 6B*). Stroke volumes and cardiac output declined to a similar extend in both groups after MI (*Figure 6B*). Heart rates after MI did not differ between both groups (*Supplemental Figure IVB*). Measurements of the left ventricular anterior wall thickness revealed thinner walls in the JZL184-treated mice, thereby confirming our histological findings (*Supplemental Figure IVC*).

3.7 Pharmacological MAGL inhibition after ischemia-reperfusion increases cardiac myeloid cell recruitment, M1 macrophage accumulation and ventricular fibrosis

Finally, we aimed to validate the effect of MAGL inhibition in a clinically more relevant

scenario and subjected mice to transient LAD occlusion with 45 min of ischemia and subsequent reperfusion or to corresponding sham operations (*Figure 7A*). Similar to the effects observed in the permanent occlusion model, JZL184 treatment resulted in higher numbers of neutrophils and Ly6C^{high} monocytes recruited to the heart 24 h after ischemia-reperfusion, while sham surgery did not or only minimally induce recruitment of these inflammatory myeloid cell subsets into the myocardium (*Figure 7B*). Concomitantly, plasma levels of neutrophil recruiting chemokine CXCL1 were significantly elevated in JZL184-treated mice compared to vehicle-treated mice 24 h after I/R (*Figure 7C*). In line with a more pronounced inflammatory response in these mice, cardiac MMP9 mRNA levels were also more increased at the same time point, whereas sham surgery resulted only in a minor increase of cardiac MMP9 mRNA levels (*Figure 7D*). Beyond the acute inflammatory phase 7 days after ischemia-reperfusion, we detected significantly more macrophages, in particular of the inflammatory M1 subset, in the myocardium of JZL184-treated mice (*Figure 7E-F*). Moreover, histological analysis of infarcted hearts 7 days after ischemia-reperfusion revealed larger ventricular scar sizes in JZL184-treated mice (*Figure 7G-H*), which is in agreement with our findings in the permanent LAD occlusion model.

4. Discussion

Over the past few years, the bone marrow has gained increasing interest as a source of myeloid cells, which infiltrate the heart after an acute MI. Under steady state, a large pool of leukocytes is stored in the bone marrow and supplies blood leukocytes at low numbers to self-maintain their numbers in the circulation. Acute MI alters this leukocyte supply chain, leading to leukocytosis and a massive infiltration of myeloid cells into the injured myocardium.²³ Damage-associated molecular patterns derived from dying cells likely contribute to the acceleration of hematopoiesis to meet the high demand of immune cells, which are required for initiating cardiac repair.²⁴ Here, we identified the endocannabinoid 2-AG/CB2 axis as a crucial modulator of myeloid cell release and cardiac recruitment after MI.

In support of a role for CB2 signaling in regulating bone marrow retention of neutrophils during steady state, we report that mice lacking CB2 have significantly lower bone marrow CXCL12 and VCAM-1 expression levels. CXCL12 released by bone marrow stromal cells is an important retention factor for immature neutrophils expressing its cognate receptor CXCR4.²⁵,²⁶ VCAM-1 in the bone marrow is expressed by stromal and endothelial cells as well as some hematopoietic cells such as macrophages.²⁷ Its major ligand is the integrin very late antigen 4

(VLA-4; $\alpha 4\beta 1$) which is expressed by neutrophils.²⁸ Thus, reduced CXCL12 and VCAM-1 expression might both contribute to enhanced neutrophil egress from the bone marrow in absence of CB2 signaling. In line with the role of CB2 in regulating myeloid cell mobilization from the bone marrow, systemic endocannabinoid administration into CB2^{-/-} mice had only little effects on myeloid cell mobilization into the circulation, whereas 2-AG induced myeloid cell release was very pronounced in WT mice.

During steady state, we found that leukocyte retention in the bone marrow is supported by high expression levels of endocannabinoid 2-AG synthesizing enzyme DAGL and low levels of its metabolizing enzyme MAGL. After MI, a dramatic change in the bone marrow expression of these enzymes occurs and in parallel 2-AG plasma levels increase, which are likely to contribute to the release of myeloid cells into the blood. In line with a previous report in an experimental model of liver injury,²⁹ we also observed an altered expression of endocannabinoid synthesizing and metabolizing enzymes as well as increased 2-AG levels in the injured myocardium 24 h after MI. This might be a direct effect of locally released inflammatory factors in the injured tissue.³⁰ Strikingly, the alterations in enzyme expression levels are much more important in the bone marrow compared to the ischemic myocardium. Although elevations of various endocannabinoids including anandamide have been reported in cardiovascular diseases,^{15,31} we found that only 2-AG levels increased in the plasma and myocardium after acute MI. The MI-induced changes in the expression of endocannabinoid 2-AG synthesizing and metabolizing enzymes were comparable in both WT and CB2^{-/-} mice. Given that global CB2 deficiency per se has multiple effects on cardiac healing responses,⁶⁻⁹ we subsequently focused only on WT mice to study the consequences of pharmacological MAGL inhibition on acute post-MI inflammation and healing.

After MI, increased sympathetic nervous system activity triggers hematopoietic stem and progenitor proliferation in the bone marrow and their release into the circulation.³² Moreover, danger signals released from ischemic myocardium into the circulation might contribute to an activation of the hematopoietic bone marrow niche.³³ Possibly these factors are also involved in the modulation of endocannabinoid enzyme expression and consequently endocannabinoid gradients between bone marrow, circulation and hearts. We provided two different experimental proofs that enhanced circulating endocannabinoid levels mediate myeloid cell mobilization in WT mice. First, at steady state systemic administration of 2-AG resulted in rapid increases of circulating leukocyte counts. Second, pharmacological inhibition of 2-AG metabolizing enzyme MAGL further upregulated MI-induced neutrophil and monocyte mobilization into the blood and their recruitment to the ischemic heart. We validated that

pharmacological MAGL inhibition at steady state resulted in approximately two-fold increased plasma 2-AG levels (data not shown), which are approximately in the range of the levels we found 24 h after MI. Several mechanisms might contribute to the enhanced cardiac leukocyte recruitment after injection of the MAGL inhibitor. Elevated systemic 2-AG levels might enhance myeloid cell mobilization from the bone marrow through a chemotactic effect, leading to increased cardiac recruitment.¹¹ Alternatively, 2-AG might promote inflammatory cytokine release in the heart as we found higher concentrations of neutrophil-recruiting CXCL1 and CXCL2 within the infarcted myocardium in MAGL inhibitor-treated mice.³⁴⁻³⁶ However, this could also be a secondary consequence of enhanced neutrophil recruitment by 2-AG-mediated chemoattraction.

The increased neutrophil and monocyte-driven inflammation and MMP9 release in response to MAGL inhibition during the early phase after MI translated into a massive infarct. In the later infarct healing phase 7 days after ischemia-reperfusion, MAGL inhibition led to increased numbers of cardiac macrophages of an inflammatory phenotype, which might be a consequence of the enhanced monocyte recruitment or a delay in inflammation resolution.³⁷ These cells are likely to contribute to an unfavorable cardiac wound healing, as observed in mice treated with JZL184. Interestingly, MAGL inhibition did not affect apoptotic cell numbers in the infarct, which could indicate that phagocytosis function, mainly promoted by M2 macrophages, is unaffected by 2-AG. The increased cardiac MMP9 protein levels in mice treated with MAGL inhibitor, associated with larger ventricular scar sizes of a poor quality, are in line with previous reports that MMP9 regulates pathologic cardiac remodeling processes.^{38, 39} In particular, reduced density of collagen type I fibers and a thinner left ventricular anterior wall thickness in MAGL inhibitor-treated mice results in fragile ventricular walls, which bear the risk of cardiac ruptures.^{40, 41} This is in line with the higher mortality and increased incidence of cardiac rupture in mice receiving MAGL inhibitor compared to the vehicle group. The observation that excessive cardiac neutrophil infiltration into the heart of MAGL inhibitor-treated mice leads to an increased infarct size, cardiac rupture and worsened cardiac function is also in agreement with our previously published findings that time-of-day-dependent fluctuations of circulating blood and tissue neutrophil counts critically affect MI healing responses.⁴⁰ Although endocannabinoid signaling per se might affect cardiovascular physiology,⁴² MAGL inhibition did not affect heart rate and cardiac output after MI. However, MAGL inhibitor-treated mice suffered from more pronounced decline of ejection fractions 3 to 21 days after MI and ventricular dilatation 14 to 21 days post-MI compared to the vehicle group.

Since timely revascularization is the gold standard of MI treatment, we aimed to verify our finding in a clinically more relevant myocardial ischemia-reperfusion MI model. This model differs from the permanent ligation MI model as revascularization after ischemia results in reperfusion injury, which originates, among other, from a massive leukocyte infiltration immediately after reopening coronary blood flow.⁴³ Similar to our findings in the permanent ligation model, MAGL inhibition after ischemia-reperfusion increased cardiac myeloid recruitment, which was accompanied by elevated plasma CXCL1 and cardiac MMP9 mRNA levels in the early inflammatory phase. Beyond the acute inflammatory phase, we noted a sustained presence of proinflammatory M1 macrophages in the myocardium and larger ventricular scar sizes. Although these preclinical observations need to be confirmed in larger animal models or clinical trials, our findings should raise awareness for the potential role of endocannabinoids in contributing to post-MI inflammation and outcome.

Finally, it has to be considered that we performed this study only in female mice, because male mice in experimental MI models have a higher incidence of mortality due to cardiac rupture. The underlying cause for this gender difference in cardiac rupture involves higher severity of inflammation, MMP activation and damage to collagen matrix in males compared to females.⁴⁴ We believe that the use of female mice with a more moderate post-MI inflammatory response, lower incidence of mortality and thus lower number of mice to be used is more suitable for studying the causal implication of the 2AG/CB2 axis in this experimental model in accordance with the 3R guidelines. Nevertheless, it is certainly of crucial importance to consider gender differences when interpreting experimental and clinical data.

To conclude, our findings suggest that alterations of endocannabinoid 2-AG signaling via CB2 cannabinoid receptors affect leukocyte counts at steady state and after myocardial infarction, which is of clinical importance as neutrophilia after myocardial infarction is associated with a higher mortality and a poorer outcome.^{45, 46} While various side effects of pharmaceutical drugs interfering with the endocannabinoid system have been reported, little is known about the effect of these drugs on the inflammatory system. Our work raises the concern that plant-derived or synthetic cannabinoids might affect leukocyte counts in patients with cardiovascular diseases thereby increasing their risk for adverse events and outcomes. Given the increasing consumption of plant derived and synthetic cannabinoids and the use of cannabinoids for a limited number of therapeutic applications, there is certainly a high interest for further investigations in this field.

Acknowledgements

CB2/- mice were kindly provided by Andreas Zimmer, Bonn, Germany. We thank Johan Duchene, Katrin Nitz, Bartolo Ferraro, Martina Rami and Donato Santovito for helpful discussions and advice regarding methodology, data analysis and statistics. We also thank Cornelia Seidl for excellent technical assistance.

Conflict of interest: None declared.

Funding

This work was supported in part by the Deutsche Forschungsgemeinschaft [STE-1053/3-1 and STE-1053/5-1 to S.S., SFB1123 TP A1 to C.W.], the European Research Council [ERC AdG 249929 to C.W.], the German Centre for Cardiovascular Research (DZHK MHA VD1.2 to C.W. and doctoral fellowship to M.J.S.), and the FöFoLe (Förderung von Forschung und Lehre) program of the Ludwig-Maximilians-University Munich (to S.S.).

References

1. Pacher P, Mechoulam R. Is lipid signaling through cannabinoid 2 receptors part of a protective system? *Prog Lipid Res* 2011;50:193-211.
2. Pereira JP, An J, Xu Y, Huang Y, Cyster JG. Cannabinoid receptor 2 mediates the retention of immature B cells in bone marrow sinusoids. *Nat Immunol* 2009;10:403-411.
3. Kondo S, Kondo H, Nakane S, Kodaka T, Tokumura A, Waku K, Sugiura T. 2-Arachidonoylglycerol, an endogenous cannabinoid receptor agonist: identification as one of the major species of monoacylglycerols in various rat tissues, and evidence for its generation through CA2+-dependent and -independent mechanisms. *FEBS Lett* 1998;429:152-156.

4. Tuma RF, Steffens S. Targeting the endocannabinoid system to limit myocardial and cerebral ischemic and reperfusion injury. *Curr Pharm Biotechnol* 2012;13:46-58.
5. De Petrocellis L, Cascio MG, Di Marzo V. The endocannabinoid system: a general view and latest additions. *Br J Pharmacol* 2004;141:765-774.
6. Defer N, Wan J, Souktani R, Escoubet B, Perier M, Caramelle P, Manin S, Deveaux V, Bourin MC, Zimmer A, Lotersztajn S, Pecker F, Pavoine C. The cannabinoid receptor type 2 promotes cardiac myocyte and fibroblast survival and protects against ischemia/reperfusion-induced cardiomyopathy. *FASEB J* 2009;23:2120-2130.
7. Duerr GD, Heinemann JC, Suchan G, Kolobara E, Wenzel D, Geisen C, Matthey M, Passe-Tietjen K, Mahmud W, Ghanem A, Tiemann K, Alferink J, Burgdorf S, Buchalla R, Zimmer A, Lutz B, Welz A, Fleischmann BK, Dewald O. The endocannabinoid-CB2 receptor axis protects the ischemic heart at the early stage of cardiomyopathy. *Basic Res Cardiol* 2014;109:425.
8. Duerr GD, Heinemann JC, Gestrich C, Heuft T, Klaas T, Keppel K, Roell W, Klein A, Zimmer A, Velten M, Kilic A, Bindila L, Lutz B, Dewald O. Impaired border zone formation and adverse remodeling after reperfused myocardial infarction in cannabinoid CB2 receptor deficient mice. *Life Sci* 2015;138:8-17.
9. Horckmans M, Bianchini M, Santovito D, Megens RTA, Springael J-Y, Negri I, Vacca M, Di Eusanio M, Moschetta A, Weber C, Duchene J, Steffens S. Pericardial Adipose Tissue Regulates Granulopoiesis, Fibrosis, and Cardiac Function After Myocardial Infarction. *Circulation* 2018;137:948-960.
10. Montecucco F, Lenglet S, Braunersreuther V, Burger F, Pelli G, Bertolotto M, Mach F, Steffens S. CB(2) cannabinoid receptor activation is cardioprotective in a mouse model of ischemia/reperfusion. *J Mol Cell Cardiol* 2009;46:612-620.
11. Miller AM, Stella N. CB2 receptor-mediated migration of immune cells: it can go either way. *Br J Pharmacol* 2008;153:299-308.
12. Nahrendorf M, Pittet MJ, Swirski FK. Monocytes: protagonists of infarct inflammation and repair after myocardial infarction. *Circulation* 2010;121:2437-2445.
13. Soehnlein O, Steffens S, Hidalgo A, Weber C. Neutrophils as protagonists and targets in chronic inflammation. *Nat Rev Immunol* 2017;17:248-261.
14. Horckmans M, Ring L, Duchene J, Santovito D, Schloss MJ, Drechsler M, Weber C, Soehnlein O, Steffens S. Neutrophils orchestrate post-myocardial infarction healing by polarizing macrophages towards a reparative phenotype. *Eur Heart J* 2017;38:187-197.
15. Weis F, Beiras-Fernandez A, Sodian R, Kaczmarek I, Reichart B, Beiras A, Schelling G, Kreth S. Substantially altered expression pattern of cannabinoid receptor 2 and activated endocannabinoid system in patients with severe heart failure. *J Mol Cell Cardiol* 2010;48:1187-1193.
16. Batkai S, Osei-Hyiaman D, Pan H, El-Assal O, Rajesh M, Mukhopadhyay P, Hong F, Harvey-White J, Jafri A, Hasko G, Huffman JW, Gao B, Kunos G, Pacher P. Cannabinoid-2 receptor mediates protection against hepatic ischemia/reperfusion injury. *FASEB J* 2007;21:1788-1800.
17. Mukhopadhyay P, Batkai S, Rajesh M, Czifra N, Harvey-White J, Hasko G, Zsengeller Z, Gerard NP, Liaudet L, Kunos G, Pacher P. Pharmacological inhibition of CB1 cannabinoid receptor protects against doxorubicin-induced cardiotoxicity. *J Am Coll Cardiol* 2007;50:528-536.
18. Buckley NE, McCoy KL, Mezey E, Bonner T, Zimmer A, Felder CC, Glass M. Immunomodulation by cannabinoids is absent in mice deficient for the cannabinoid CB(2) receptor. *Eur J Pharmacol* 2000;396:141-149.
19. Panikashvili D, Simeonidou C, Ben-Shabat S, Hanus L, Breuer A, Mechoulam R, Shohami E. An endogenous cannabinoid (2-AG) is neuroprotective after brain injury. *Nature* 2001;413:527-531.

20. Schneider CA, Rasband WS, Eliceiri KW. NIH Image to ImageJ: 25 years of image analysis. *Nature Methods* 2012;**9**:671.
21. Thomas A, Hopfgartner G, Giroud C, Staub C. Quantitative and qualitative profiling of endocannabinoids in human plasma using a triple quadrupole linear ion trap mass spectrometer with liquid chromatography. *Rapid Commun Mass Spectrom* 2009;**23**:629-638.
22. Quercioli A, Montecucco F, Pataky Z, Thomas A, Ambrosio G, Staub C, Di Marzo V, Ratib O, Mach F, Golay A, Schindler TH. Improvement in coronary circulatory function in morbidly obese individuals after gastric bypass-induced weight loss: relation to alterations in endocannabinoids and adipocytokines. *Eur Heart J* 2013;**34**:2063-2073.
23. Nahrendorf M, Swirski FK. Innate immune cells in ischaemic heart disease: does myocardial infarction beget myocardial infarction? *Eur Heart J* 2016;**37**:868-872.
24. Epelman S, Liu PP, Mann DL. Role of innate and adaptive immune mechanisms in cardiac injury and repair. *Nat Rev Immunol* 2015;**15**:117-129.
25. Eash KJ, Greenbaum AM, Gopalan PK, Link DC. CXCR2 and CXCR4 antagonistically regulate neutrophil trafficking from murine bone marrow. *J Clin Invest* 2010;**120**:2423-2431.
26. Eash KJ, Means JM, White DW, Link DC. CXCR4 is a key regulator of neutrophil release from the bone marrow under basal and stress granulopoiesis conditions. *Blood* 2009;**113**:4711-4719.
27. Ulyanova T, Scott LM, Priestley GV, Jiang Y, Nakamoto B, Koni PA, Papayannopoulou T. VCAM-1 expression in adult hematopoietic and nonhematopoietic cells is controlled by tissue-inductive signals and reflects their developmental origin. *Blood* 2005;**106**:86-94.
28. Pereira S, Zhou M, Mocsai A, Lowell C. Resting murine neutrophils express functional alpha 4 integrins that signal through Src family kinases. *J Immunol* 2001;**166**:4115-4123.
29. Mai P, Yang L, Tian L, Wang L, Jia S, Zhang Y, Liu X, Yang L, Li L. Endocannabinoid System Contributes to Liver Injury and Inflammation by Activation of Bone Marrow-Derived Monocytes/Macrophages in a CB1-Dependent Manner. *J Immunol* 2015;**195**:3390-3401.
30. Szafran B, Borazjani A, Lee JH, Ross MK, Kaplan BL. Lipopolysaccharide suppresses carboxylesterase 2g activity and 2-arachidonoylglycerol hydrolysis: A possible mechanism to regulate inflammation. *Prostaglandins Other Lipid Mediat* 2015;**121**:199-206.
31. Sugamura K, Sugiyama S, Nozaki T, Matsuzawa Y, Izumiya Y, Miyata K, Nakayama M, Kaikita K, Obata T, Takeya M, Ogawa H. Activated endocannabinoid system in coronary artery disease and antiinflammatory effects of cannabinoid 1 receptor blockade on macrophages. *Circulation* 2009;**119**:28-36.
32. Dutta P, Courties G, Wei Y, Leuschner F, Gorbatov R, Robbins CS, Iwamoto Y, Thompson B, Carlson AL, Heidt T, Majmudar MD, Lasitschka F, Etzrodt M, Waterman P, Waring MT, Chicoine AT, van der Laan AM, Niessen HW, Piek JJ, Rubin BB, Butany J, Stone JR, Katus HA, Murphy SA, Morrow DA, Sabatine MS, Vinegoni C, Moskowitz MA, Pittet MJ, Libby P, Lin CP, Swirski FK, Weissleder R, Nahrendorf M. Myocardial infarction accelerates atherosclerosis. *Nature* 2012;**487**:325-329.
33. van Hout GP, Arslan F, Pasterkamp G, Hoefer IE. Targeting danger-associated molecular patterns after myocardial infarction. *Expert Opin Ther Targets* 2016;**20**:223-239.
34. Leung BP, Culshaw S, Gracie JA, Hunter D, Canetti CA, Campbell C, Cunha F, Liew FY, McInnes IB. A role for IL-18 in neutrophil activation. *J Immunol* 2001;**167**:2879-2886.

35. Bonecchi R, Facchetti F, Dusi S, Luini W, Lissandrini D, Simmelink M, Locati M, Bernasconi S, Allavena P, Brandt E, Rossi F, Mantovani A, Sozzani S. Induction of functional IL-8 receptors by IL-4 and IL-13 in human monocytes. *J Immunol* 2000;164:3862-3869.
36. Montecucco F, Steffens S, Burger F, Da Costa A, Bianchi G, Bertolotto M, Mach F, Dallegrì F, Ottonello L. Tumor necrosis factor-alpha (TNF-alpha) induces integrin CD11b/CD18 (Mac-1) up-regulation and migration to the CC chemokine CCL3 (MIP-1alpha) on human neutrophils through defined signalling pathways. *Cell Signal* 2008;20:557-568.
37. Hulsmans M, Sam F, Nahrendorf M. Monocyte and macrophage contributions to cardiac remodeling. *Journal of Molecular and Cellular Cardiology* 2016;93:149-155.
38. Iyer RP, de Castro Bras LE, Patterson NL, Bhowmick M, Flynn ER, Asher M, Cannon PL, Deleon-Pennell KY, Fields GB, Lindsey ML. Early matrix metalloproteinase-9 inhibition post-myocardial infarction worsens cardiac dysfunction by delaying inflammation resolution. *J Mol Cell Cardiol* 2016;100:109-117.
39. Yabluchanskiy A, Ma Y, Iyer RP, Hall ME, Lindsey ML. Matrix Metalloproteinase-9: Many Shades of Function in Cardiovascular Disease. *Physiology* 2013;28:391-403.
40. Schloss MJ, Horckmans M, Nitz K, Duchene J, Drechsler M, Bidzhekov K, Scheiermann C, Weber C, Soehnlein O, Steffens S. The time-of-day of myocardial infarction onset affects healing through oscillations in cardiac neutrophil recruitment. *EMBO Mol Med* 2016;8:937-948.
41. Kong P, Christia P, Frangogiannis NG. The pathogenesis of cardiac fibrosis. *Cell Mol Life Sci* 2014;71:549-574.
42. Pacher P, Steffens S, Hasko G, Schindler TH, Kunos G. Cardiovascular effects of marijuana and synthetic cannabinoids: the good, the bad, and the ugly. *Nat Rev Cardiol* 2018;15:151-166.
43. Frohlich GM, Meier P, White SK, Yellon DM, Hausenloy DJ. Myocardial reperfusion injury: looking beyond primary PCI. *Eur Heart J* 2013;34:1714-1722.
44. Fang L, Gao XM, Moore XL, Kiriazis H, Su Y, Ming Z, Lim YL, Dart AM, Du XJ. Differences in inflammation, MMP activation and collagen damage account for gender difference in murine cardiac rupture following myocardial infarction. *J Mol Cell Cardiol* 2007;43:535-544.
45. Kyne L, Hausdorff JM, Knight E, Dukas L, Azhar G, Wei JY. Neutrophilia and congestive heart failure after acute myocardial infarction. *Am Heart J* 2000;139:94-100.
46. Chia S, Nagurney JT, Brown DF, Raffel OC, Bamberg F, Senatore F, Wackers FJ, Jang IK. Association of leukocyte and neutrophil counts with infarct size, left ventricular function and outcomes after percutaneous coronary intervention for ST-elevation myocardial infarction. *Am J Cardiol* 2009;103:333-337.

Figure legends

Figure 1. The endocannabinoid 2-AG/CB2 receptor axis promotes leukocyte mobilization. A, Representative flow cytometry plots and (B) blood counts of WT and CB2^{-/-} mice before and 2 h after intravenous (i.v.) 2-AG bolus injections. Symbols indicate individual mice ($n = 6$); paired student's *t*-test; * $P < 0.05$; ns, not significant.

Figure 2. MI inverts bone marrow and cardiac expression profiles of endocannabinoid biosynthesis and degradation pathways. Levels of anandamide (AEA), palmitoylethanolamide (PEA), oleoylethanolamine (OEA), and 2-arachidonoylglycerol (2-AG) in plasma (A) and heart (B) at steady state and 24 h after MI in WT mice. Messenger RNA levels of endocannabinoid synthesizing enzyme DAGL β and metabolizing enzyme MAGL in heart (C) and bone marrow (D) at steady state and 24 h after MI in WT mice. Enzyme mRNA levels were normalized to HPRT and the fold change after MI compared to baseline (no MI) was calculated for each genotype. All data are mean \pm SEM ($n = 6$ -10 mice); two-way ANOVA followed by Bonferroni *post hoc* test (A-C) or unpaired student's *t*-test (D-E); * $P < 0.05$; ns, not significant.

Figure 3. Pharmacological MAGL inhibition enhances cardiac leukocyte recruitment and inflammation after MI. A, Permanent LAD occlusion was performed in WT mice receiving intraperitoneal injection of vehicle (DMSO) or MAGL inhibitor (JZL184) 24 h before surgery. B, Blood counts of granulocytes and monocytes 24 h after MI ($n = 9$ -11). C, Flow cytometric quantification of neutrophils and Ly6C^{high} monocytes in digested hearts 24 h after MI ($n = 6$). D, Protein levels of pro-inflammatory chemokines within the infarcted myocardium 24 h after MI ($n = 8$ -9 mice). E-F, Western blot analysis of cardiac MMP9 (active form) and GAPDH 24 h after MI and quantification of MMP9 band density, normalized to GAPDH and shown as arbitrary units (a.u.) relative to the vehicle group (set to 100; $n = 7$ -8 mice). G-H, Plasma levels of pro-inflammatory cytokines ($n = 5$ -7) and chemokines 24 h after MI ($n = 6$ -7 mice). Data were obtained in two independent experiments. All data are mean \pm SEM; unpaired student's *t*-test; * $P < 0.05$.

Figure 4. Pharmacological MAGL inhibition increases infarct size and mortality. A, Permanent LAD occlusion was performed in WT mice receiving either vehicle (DMSO) or MAGL inhibitor (JZL184) intraperitoneally 24 h before and subsequently every 48 h until harvest. B, TTC staining (yellow, infarct; red, vital myocardium) and quantification of infarct size

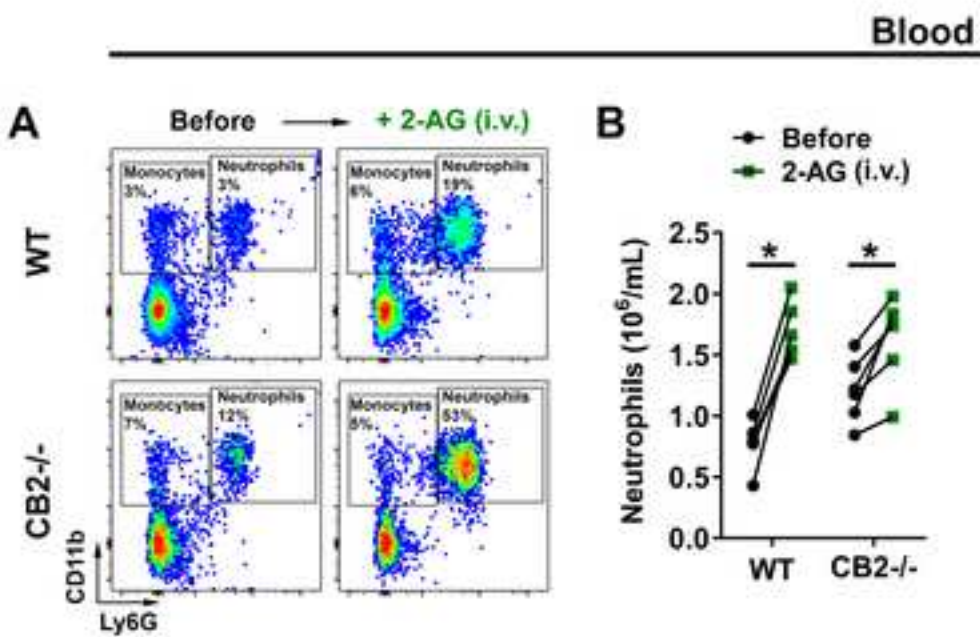
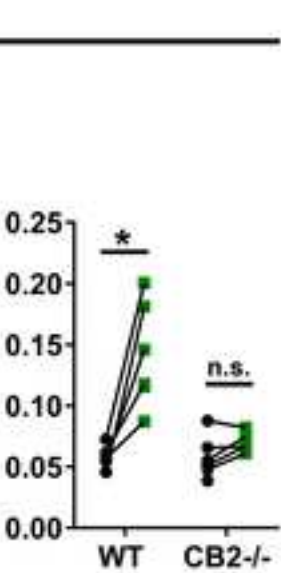
normalized to the left ventricle (LV; $n = 6$ -8 mice). C, Plasma troponin I levels 24 h after MI ($n = 19$ mice). B-C, Data are mean \pm SEM; unpaired student's *t*-test. D, Survival rates after MI (total $n = 68$ mice) and (E) cause of death. Statistical significance was determined using a log-rank test. All data were obtained in at least two independent experiments; * $P < 0.05$.

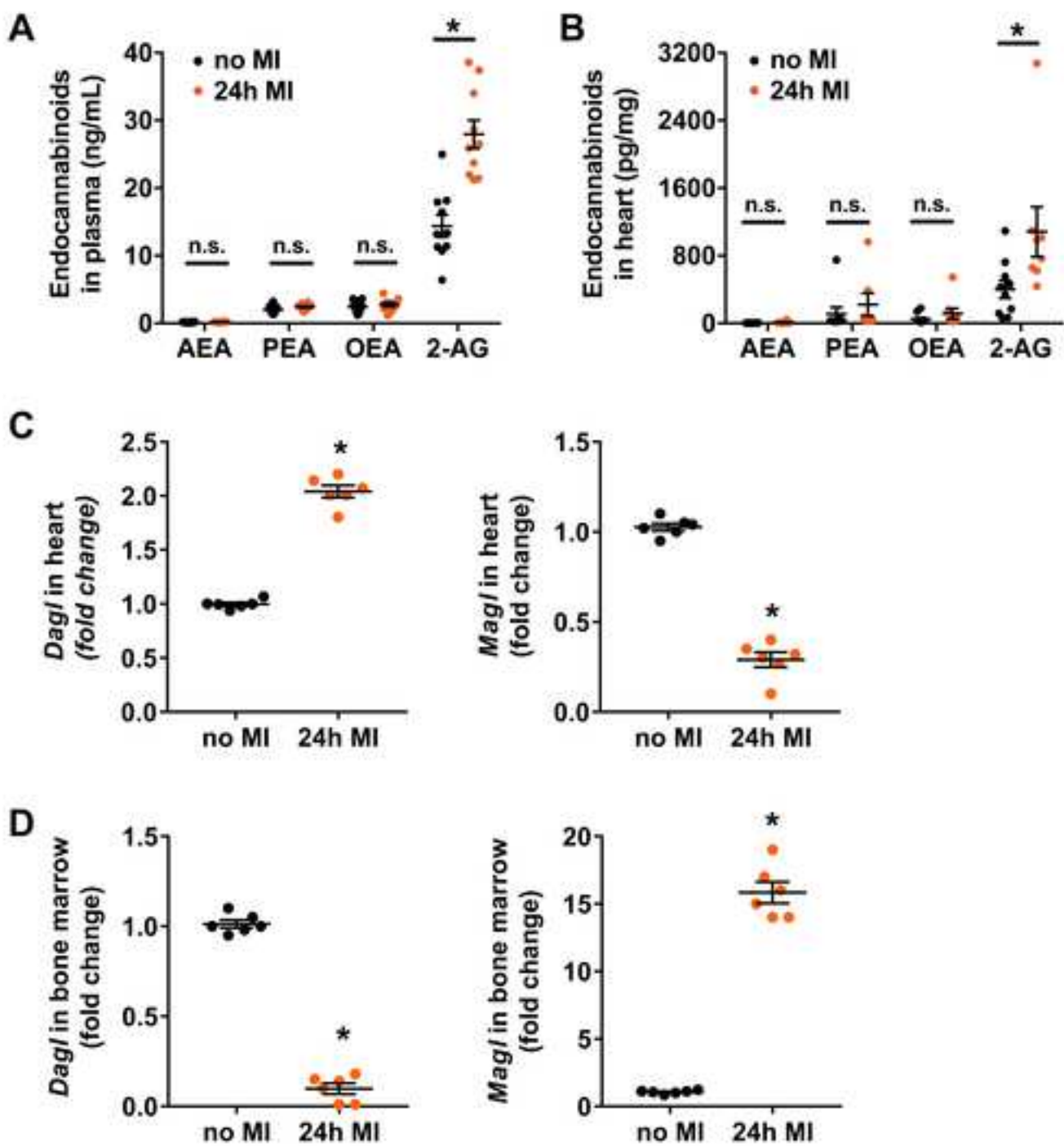
Figure 5. Pharmacological MAGL inhibition impairs ventricular remodeling 7d after MI. Permanent LAD occlusion was performed in WT mice receiving either vehicle (DMSO) or MAGL inhibitor (JZL184) intraperitoneally 24 h before and subsequently every 48 h until harvest. A, Representative TUNEL staining of the infarcted myocardium of DMSO- and JZL184-treated mice 7 days after myocardial infarction (blue, nuclei; green, TUNEL; 10x magnification; scale bars represent 800 μ m). B, Quantification of TUNEL-positive area within the infarcted area. C, Masson's trichrome staining of fibrosis (blue, collagen; red, vital myocardium; 20x magnification; scale bars represent 80 μ m). D, Quantification of fibrotic scar size relative to total left ventricular (LV) area and quantification of the LV anterior wall thickness of the fibrotic scar. E, Representative bright field (left) and corresponding polarized light images (right) of Sirius-Red staining identifying collagen type I fibers as red-yellow fibers and collagen type III fibers as green fibers within the infarct area (20x magnification; scale bars represent 80 μ m). F, Quantification of collagen type I positive area and collagen type III positive area within the infarcted area. Data were obtained in two independent experiments ($n = 6$ -9 mice in total). All data are mean \pm SEM; unpaired student's *t*-test; * $P < 0.05$.

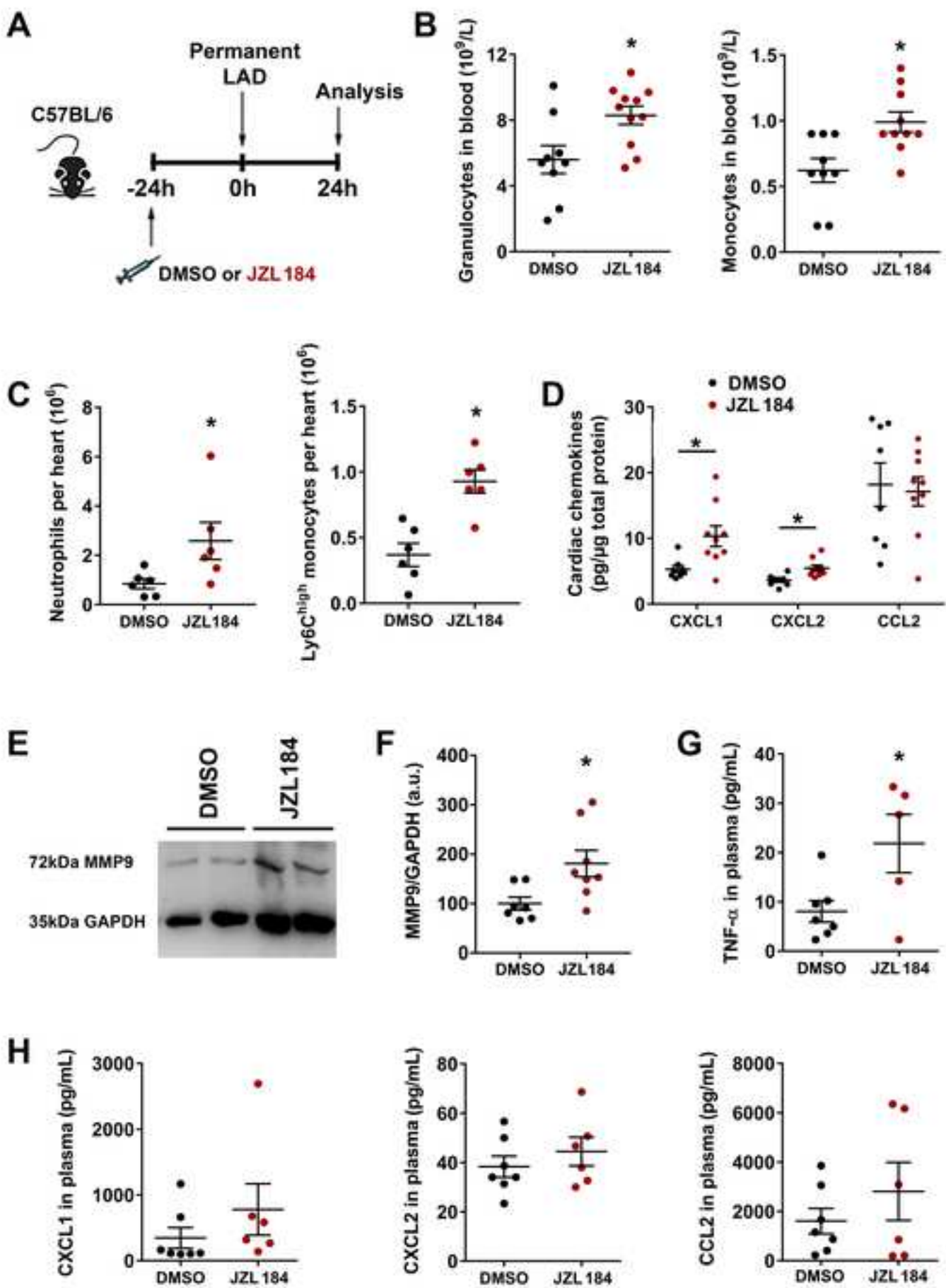
Figure 6. Pharmacological MAGL-inhibition worsens cardiac function after MI. Permanent LAD occlusion was performed in WT mice receiving either vehicle (DMSO) or MAGL inhibitor (JZL184) intraperitoneally 24 h before and subsequently every 48 h until harvest. A, Representative vector diagrams showing the direction and magnitude of myocardial contraction at midsystole. Representative three-dimensional regional wall displacement illustrations showing contraction (positive values, yellow-red) or relaxation (negative values, blue) of consecutive cardiac cycle results. B, Echocardiographic assessment of cardiac function parameters and left ventricular diameters after MI. Data were obtained in three independent experiments ($n = 12$ -15 mice in total). All data are mean \pm SEM; two-way ANOVA followed by Bonferroni *post hoc* test; * $P < 0.05$.

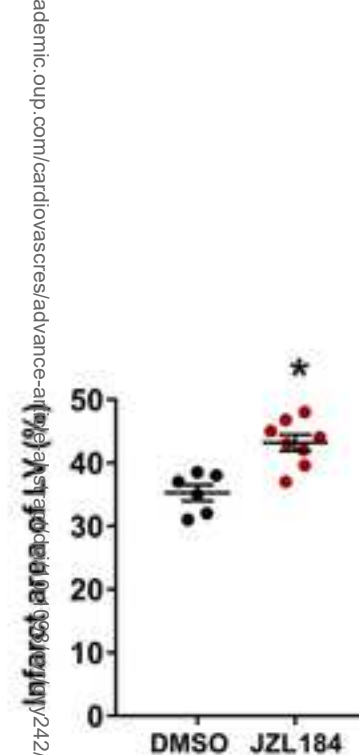
Figure 7. Pharmacological MAGL inhibition increases cardiac myeloid cell recruitment and ventricular fibrosis after myocardial ischemia-reperfusion. A, 45 minutes of

myocardial ischemia followed by reperfusion or corresponding sham operations were performed in WT mice receiving either vehicle (DMSO) or MAGL inhibitor (JZL184) intraperitoneally 24 h before and subsequently every 48 h until harvest. B, Flow cytometric quantification of neutrophils and Ly6C^{high} monocytes in digested hearts 24 h after ischemia-reperfusion or sham operation ($n = 6$ -13 mice). C, Plasma levels of the pro-inflammatory cytokine CXCL1 24 h after I/R ($n = 6$ mice). D, MMP9 mRNA expression within the infarcted myocardium 24 h after ischemia-reperfusion or the corresponding myocardium of sham operated mice normalized to HPRT and shown as fold change to steady state myocardium (The dotted line indicates steady state levels; $n = 6$ mice). E, Flow cytometric quantification of macrophages in digested hearts 7 days after ischemia-reperfusion ($n = 6$ mice). F, Pie chart of the ratio between inflammatory macrophages (M1 MΦ; CD206-) and reparative macrophages (M2 MΦ; CD206+) 7 days after ischemia-reperfusion ($n = 6$ mice). G, Representative images 7 days after ischemia-reperfusion stained with Masson trichrome (blue, collagen; red, vital myocardium; 20x magnification; scale bars represent 50 μ m). H, Quantification of fibrotic scar size relative to total left ventricular (LV) area 7 days after ischemia-reperfusion ($n = 6$ mice). Data were obtained in two independent experiments. All data are mean \pm SEM; unpaired student's *t*-test; * $P < 0.05$; two-way ANOVA followed by Bonferroni *post hoc* test (B, D) or unpaired student's *t*-test (C, E, F, H); * $P < 0.05$; ns, not significant.









academic.oup.com/cardiovascres/advance-article-abstract/24/2/5115994 by Université de Genève and EPFL Lausanne user on 09 October 2018

